Nonsmooth modal analysis from elementary impact oscillators to turbomachines: limitations and avenues

Anders Thorin, Mathias Legrand

Nonsmooth modal analysis from elementary impact oscillators to turbomachines: limitations and avenues

Anders Thorin, Mathias Legrand

ISROMAC 2016

International Symposium on Transport Phenomena and Dynamics of Rotating Machinery

Hawaii, Honolulu

April 10-15, 2016

Abstract

In mechanical engineering, nonlinear modes characterise the behaviour of nonlinear vibratory systems. In the current state-of-the-art, they are well defined for smooth nonlinear systems (of moderate size) of Ordinary Differential Equations governing the dynamics. They are defined as continua of periodic orbits forming two-dimensional invariant manifolds in the state space. This framework has lately been extended to nonsmooth mechanical systems involving impact dynamics.

From the theoretical standpoint, strong mathematical results about existence, uniqueness and analytical or approximate equations of nonsmooth modes have recently been established on a linear spring-mass chain undergoing a Newton elastic impact law on one of its masses. From the industrial point of view, their application is not straightforward. This paper investigates the possibilities and the limitations of these tools with a practical end: the issue of blade–casing unilateral contact interactions in turbomachines.

The main differences between a simple spring-mass chain and complex blade–casing models are investigated point by point: non-diagonal mass matrix, geometrical differences, scalability for thousands of degrees of freedom, convergence with respect to the number of dofs, stability and relationships with force and damped mechanical systems.

It is found that the proposed formulation and corresponding solutions apply to very general spring-mass systems, involving non-diagonal mass matrices and non-tridiagonal stiffness matrices, opening avenues to investigate complex industrial systems. However, the relationship between the forced and damped behaviour and nonsmooth modes is not fully understood yet.

Keywords

Nonlinear modal analysis — nonsmooth dynamics — blade–casing contact interaction

Mechanical Engineering, McGill University, Montreal, Canada

INTRODUCTION

Nonlinear modes of vibration provide useful means of investigating the dynamics of nonlinear systems [1]. They can be defined as a two-dimensional continuum of periodic trajectories lying on *invariant manifolds* in the state space, whose coordinates are the chosen generalised coordinates and generalised velocities. The "invariant"' property refers to the fact that if the state of a mechanical system is on its nonlinear mode at a given time, it will remain on it as time unfolds. Thus, nonlinear modes are particular surfaces in the state space which characterise, locally, the behaviour of a dynamical system.

For smooth nonlinear systems, nonlinear modes can be approximated locally by choosing a pair of master coordinates [2, 3], writing the generalised coordinates and velocities as unknown functions of this pair and calculating a Taylor expansion of these unknown functions. This results in a parametric equation formulated in the pair of master coordinates, yielding one two-dimensional surface in the state space: a nonlinear mode.

A considerable limitation of this method is that it relies on the smoothness of the differential equations (ODEs) and no longer applies to nonsmooth mechanical systems, *i.e.* systems undergoing impact or dry friction. Yet, many vibratory systems undergo unilateral contact conditions such as the common blade–casing contact occurrences in turbomachines. The operating clearance between blades and surrounding casing has to be as small as possible for efficiency purposes, potentially initiating contact induced vibratory phenomena [4]. Because of the velocity discontinuities induced by impacts, such events are no longer captured by ODEs and require more complex mathematical tools such as linear complementary conditions, inclusions in cones, inclusions of differential measures or variational inequalities [5]. Modal analysis is currently unable to properly handle such systems.

A simple spring-mass oscillator has been recently studied [6, 7]. The oscillator is subject to unilateral contact with a Newton impact law: $v(t_{\text{imp}}^{+}) = -v(t_{\text{imp}}^{-})$ where t_{imp} is any time of impact, $v(t_{\text{imp}}^{-})$ is the pre-impact velocity and $v(t_{\text{imp}}^{+})$ is the post-impact velocity. The number of impact(s) per period arises a as a natural criterion for the classification of nonsmooth modes. Periodic solutions with one impact per period (ipp) have been thoroughly investigated in [6], leading to 1 ipp nonsmooth-modes. In [7], a formulation for 2 ipp is proposed. More general results for n dof and k ipp have been found and will be published soon.

This contribution targets the implementation of modal

analysis in the framework of rotating machinery where unilateral contact events are known to emerge. It focuses on current challenges and limitation by paying attention to simple qualitative behaviours. Questions of interest are the theoretical and practical applicability of nonsmooth modes to generic mechanical systems featuring potential large arbitrary mass and stiffness matrices.

The main mathematical results, unpublished yet, of nonsmooth modal analysis for a spring-mass chain are provided in Section 1. They serve as a starting point for the present study and a basic example is proposed for illustrative purposes. In Section 2, the main steps required to extend the results to a full blade-casing contact model are identified and investigated.

1. STARTING POINT: MATHEMATICAL RESULTS

In this section, the main mathematical results about nonsmooth modes are given. For the sake of conciseness, only the main ingredients are listed in a quite abstract fashion, limiting the presentation to the important results. In substance, the latter prove existence and uniqueness, under some conditions, of periodic solutions to the problem described in subsection 1.1 for k impact(s) per period. They also yield an analytical ($k = 1$) or approximate ($k \geq 2$) expressions of the nonsmooth modes.

1.1 Model and dynamical equations

Consider the spring-mass system in Fig. 1. The quantities m_i

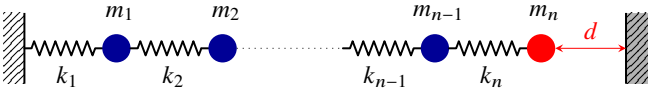

Figure 1. Base model for the study of nonsmooth modes.

are masses and k_i are stiffnesses. The position of the mass i is stored in x_i and by convention $x_i = 0$ at rest, for $i \in [\![1, n]\!]$. The position x_n of the last mass is constrained by an obstacle located at position d, which is described mathematically by the following Signorini condition such that $\forall t \geq 0$:

$$d - x_n(t) \geq 0 \tag{1a}$$
$$\lambda(t) \geq 0 \tag{1b}$$
$$\lambda(t)(d - x_n(t)) = 0 \tag{1c}$$

This unilateral condition has to be supplemented by an impact law between the n-th mass and the obstacle: to this end, the simple Newton impact law is selected so that the overall dynamics writes:

$$\forall t, \quad d - x_n(t) \geq 0 \tag{2a}$$
$$\forall t \text{ such that } x_n(t) < d, \quad \mathbf{M}\ddot{\mathbf{x}} + \mathbf{K}\mathbf{x} = \mathbf{0} \tag{2b}$$
$$\forall t \text{ such that } x_n(t) = d, \quad \dot{x}_n(t^+) = -\dot{x}_n(t^-) \tag{2c}$$

with the mass matrix $\mathbf{M} = \mathrm{diag}(m_1, \ldots, m_n)$, the stiffness matrix $\mathbf{K} = \mathrm{tridiag}(-k_{i-1}, k_{i-1} + k_i, -k_i)$ and the vector of positions $\mathbf{x} = [x_1, \ldots, x_n]^\top$.

1.2 Preliminary definitions

Let us define:

- $\mathbf{B} = -(\sqrt{\mathbf{M}})^{-1}\sqrt{\mathbf{K}}$; $\mathbf{Q}$ an orthogonal matrix such that $\mathbf{B}\mathbf{B}^\top = \mathbf{Q}\boldsymbol{\Delta}^2\mathbf{Q}^{-1}$ with $\boldsymbol{\Delta}$ a diagonal matrix; $\omega_i > 0$ the element (i, i) of $\boldsymbol{\Delta}$.
- k the number of impacts per period and $t_1, \ldots, t_k$ the instants of impacts. The duration between two successive impacts denoted by $\sigma_i = t_i - t_{i-1}$ with $t_0 = 0$.
- The period T; as by convention contact is activated at $t = 0$, the period is equal to the time of the k-th impact: $T = t_k$.
- The function

$$Q_T(\sigma) = \sum_{i=1}^{n} \frac{\sin(\omega_i \sigma/2)}{\sin(\omega_i T/2)} {q_{n,j}}^2 \tag{3}$$

  where $q_{n,j}$ is the element (n, j) of $\mathbf{Q}$.
- The following vectors:

$$\mathbf{W}_n = -\frac{1}{\sqrt{m_n}} \begin{bmatrix} q_{n,1}/\omega_1 \\ 0 \\ \vdots \\ q_{n,n}/\omega_n \\ 0 \end{bmatrix} \qquad \mathbf{R} = -\frac{1}{\sqrt{m_n}} \begin{bmatrix} q_{n,1} \\ 0 \\ \vdots \\ q_{n,n} \\ 0 \end{bmatrix} \tag{4}$$

- The matrix exponential

$$\mathbf{S}(t) = \exp\left(t \begin{bmatrix} \mathbf{0} & \mathbf{I} \\ -\mathbf{M}^{-1}\mathbf{K} & \mathbf{0} \end{bmatrix} \right) \tag{5}$$

- The skew-symmetric matrix $\boldsymbol{\Pi}$ populated by

$$\Pi_{ij}(t_1, \ldots, t_k) = Q_T(2(t_j - t_i) - T) \tag{6}$$

  for $i < j \leq k$.
- The symmetric matrix $\boldsymbol{\Sigma}$ populated by the elements

$$\Sigma_{ij}(t_1, \ldots, t_k) = 2\mathbf{W}_n^\top (\mathbf{S}(\tfrac{T}{2}) - \mathbf{S}(-\tfrac{T}{2})^{-1}\mathbf{S}(t_i - t_j + \tfrac{T}{2})\mathbf{R} \tag{7}$$

  for $i < j \leq k$.
- The constant vector $\mathbf{j} = [1, \ldots, 1]^\top \in \mathbb{R}^k$.

1.3 Mathematical results

A necessary condition for the existence of a periodic solution with k ipp is that there exists a $\boldsymbol{\lambda} \in \mathbb{R}^k$ such that:

$$\boldsymbol{\Pi}(t_1, \ldots, t_k)\boldsymbol{\lambda} = \mathbf{0} \tag{8}$$
$$\boldsymbol{\Sigma}(t_1, \ldots, t_k)\boldsymbol{\lambda} = d\mathbf{j} \tag{9}$$

If such a condition is satisfied, then let us define:

$$\phi_{p,T}(\sigma) = -\frac{1}{\sqrt{m_p}} \sum_{j=1}^{n} \frac{\cos(\omega_j \sigma/2)}{\omega_j \sin(\omega_j T/2)} q_{p,j} q_{n,j} \tag{10}$$

and

$$\psi_{p,T}(\sigma) = 2\frac{\mathrm{d}\phi_{p,T}}{\mathrm{d}t}(t) = \frac{1}{\sqrt{m_p}} \sum_{j=1}^{n} \frac{\sin(\omega_j \sigma/2)}{\sin(\omega_j T/2)} q_{p,j} q_{n,j}$$

(11)

Also, consider $\forall \tau \in [0, \sigma_{i+1}]$ the p-th position:

$$x_p(\tau + t_i) = \sum_{j=1}^{i} \lambda_j \phi_{p,\sigma}(2(\tau + t_i - t_j) - T) + \sum_{j=i+1}^{k} \lambda_j \phi_{p,\sigma}(2(\tau + t_i - t_j) + T) \tag{12}$$

If $\forall i \in [\![1, k]\!]$, $\forall \tau \in [0, \sigma_{i+1}]$, $x_n(\tau + \sigma_{i+1}) \leq d$, then $\mathbf{x}$ is a periodic solution of problem (2) with k impact times $t_1, \ldots, t_k$. The velocity p is given $\forall \tau \in [0, \sigma_{i+1}]$ by

$$y_p(\tau + t_i) = \sum_{j=1}^{i} \lambda_j \psi_{p,T}(2(\tau + t_i - t_j) - T) + \sum_{j=i+1}^{k} \lambda_j \psi_{p,\sigma}(2(\tau + t_i - t_j) + T) \tag{13}$$

1.4 Example

For illustration purposes, arbitrary choices $n = 2$ and $k = 2$ are made with $k_1 = k_2 = 1$ and $m_1 = m_2 = 1/2$. The definition of matrix Π, see Eq. (6), with $t_2 = T$ leads to

$$\Pi(t_1, T) = \begin{bmatrix} 0 & Q_T(T - 2t_1) \\ -Q_T(T - 2t_1) & 0 \end{bmatrix} \tag{14}$$

Condition (8) yields either the trivial solution $\boldsymbol{\lambda} = \mathbf{0}$ or the more interesting equation

$$Q_T(T - 2t_1) = 0 \tag{15}$$

From the definition of Q_T given in Eq. (3), and the eigenfrequencies of the system ω_1, ω_2, it is possible to approximate (t_1, T) solution of (15). Note that the resonant cases are excluded ($(t_1, T \notin \{\frac{2\pi}{\omega_1}, \frac{2\pi}{\omega_2}\}$). The roots of the numerator of $Q_T(T - 2t_1)$ is displayed in Fig. 2. To correctly interpret Eq. (8), is has to be understood that 2 ipp motions do not exist for any (t_1, T). Eq. (8) gives a necessary (but not sufficient) condition for the existence of such solutions. Note that the line of equation $T - t_1 = t_1$ in Fig. 2 corresponds to 1 ipp motions of period $T/2$ but seen as T-periodic motions.

For chosen (t_1, t_2) satisfying Eq. (8), Eq. (9) yields the values of the vector $\boldsymbol{\lambda}$. This forces the impact conditions at t_1 and t_2 to coincide with $x_n = d$. The relation between the positions x_p and the components of $\boldsymbol{\lambda}$ is in Eq. (12).

Both conditions (8) and (9) are not sufficient: among the motions they lead to, they do not exclude those which can violate the constraint $x_n \leq d$. This condition has to be tested numerically using Eq. (12). If it is fulfilled, then the corresponding $\mathbf{x}$ is a solution. By continuity, there are other solutions in the neighbourhood of the selected (t_1, T), yielding a continuum of periodic trajectories with two impacts per period. Samples of the continuum are plotted in Fig. 3, corresponding to points chosen on the red curve of Fig. 2. This continuum of solutions can also be represented as an invariant manifold, gathering the continuum of periodic orbits in the state state. This two-dimensional object, embedded in a $2n$ dimensional state space (n positions, n velocities) can be projected into the three-dimensional space $(x_1, x_2, \dot{x}_2)$. Such a projection is represented in Fig. 4. This example was used to illustrate the mathematical results and show, in practice, how they lead to the construction of nonsmooth modes for the spring-mass chain system of Fig. 1. The next part consists in exploring the applicability of these developments to more challenging models such as a blade–casing model of a turbomachine.

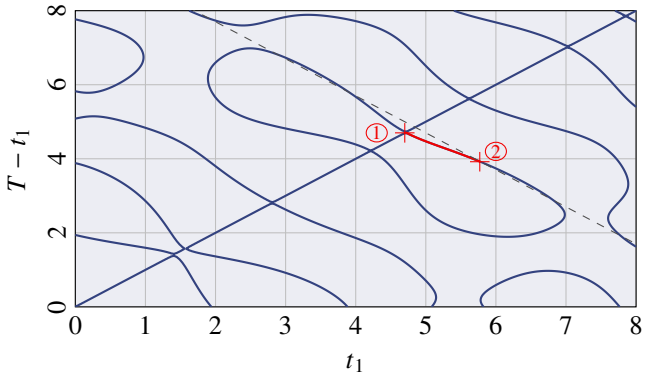

Figure 2. Numerically calculated roots of the numerator of $Q_T(T - 2t_1)$. In red: continuum of solutions corresponding to Fig. 3 and 4. Dashed line: $T = 5T_2$ where $T_2 = 2\pi/\omega_2$ is the second eigenfrequency.

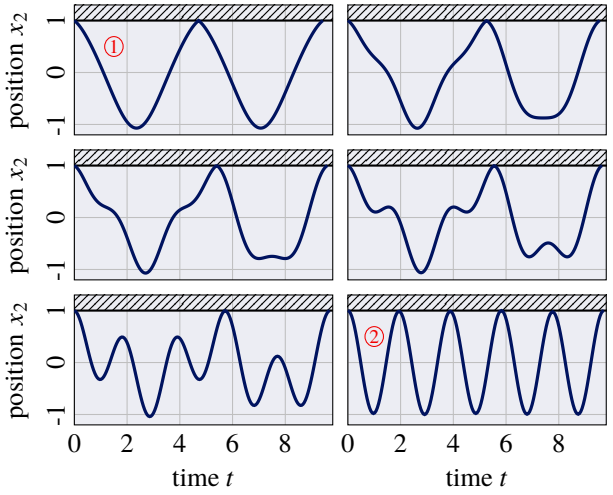

Figure 3. Example of periodic trajectories with two impacts per period. They correspond the red curve parametrised by (t_1, T) on Fig. 2 and delimited by ① and ②. ① corresponds to a 1 ipp trajectory taken on two impacts. ② corresponds to the fifth harmonic of the second linear mode. In between are purely 2 ipp motions.

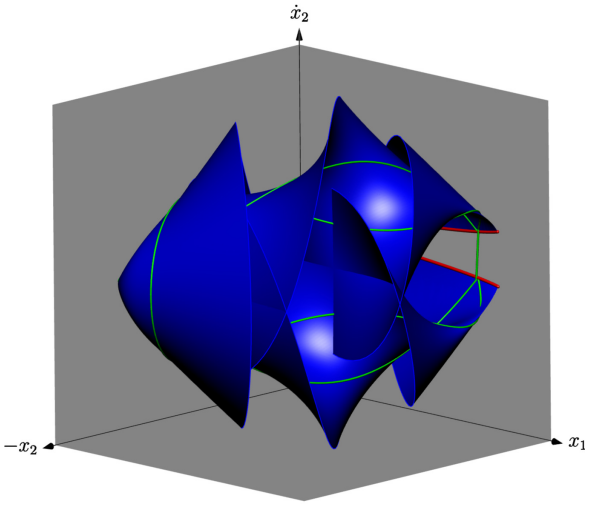

Figure 4. Example of nonsmooth mode corresponding to (t_1, T) on the red curve of Fig. 2. The green curve corresponds to an periodic solution of the nonsmooth dynamics. The red curve highlights the velocity discontinuities occurring when $x_2 = d$.

2. GENERIC MECHANICAL SYSTEMS

Though very fruitful, these results were proven for the spring-mass system of Fig. 1. FEM models used for turbomachines differ from such a simple model: they involve *a priori* non-diagonal mass matrices, contain thousands of degrees-of-freedom, target much more complicated geometry involving more than two connexion per element, etc. making this method not directly applicable. These points are discussed in the present part. Nevertheless, contact is assumed to occur only on one node.

In all the computations, $k = 1$, $m = 1/N$ and $d = 1$.

2.1 Non-diagonal mass matrices

For linear spring-mass systems, the equations governing the dynamics of every degree-of-freedom can be gathered in a matrix form with a diagonal mass matrix. When dealing with finite-elements, this property is no longer conserved: basis functions are in general not orthogonal (for the canonical scalar product), yielding off-diagonal terms. However, the mass matrix remains symmetric[1]. During phases of free flight ($x_n < d$), this symmetry does not invalidate the results of Section 1. Since the proof is not given, the reader will not be able to verify this statement; the key idea is that the mass matrix is a real symmetric matrix, so is diagonalisable in an orthogonal basis. But t no longer holds for the Newton impact law: the transformation ${v_n}^+ = -{v_n}^-$ corresponds to a reflection matrix $\mathbf{N} = \mathrm{diag}(1, \ldots, 1, -1)$ of size $2n$ which is an isometry for the energy if and only if $M_{nj} = 0$ for all $j \neq n$. In other words, the Newton impact does not preserve energy if the mass which impacts the obstacle is not punctual. This is not a severe restriction. Nevertheless, our first investigations on defining an elastic impact law as an isometry for the energy and a orthogonal symmetry with respect to an hyperplane of the state space are promising and could raise this restriction. This is a complicated topic on itself and is not discussed here. Also, note that non-diagonal mass matrix are commonly *lumped* resulting in a diagonal mass matrix.

[1]The symmetry of the mass matrix can be proven with Maxwell–Betti's theorem.

2.2 Geometry of the mechanical system

Here, it is shown that the results of Section 1 apply for more complex geometries than that of Fig. 1. Two changes of geometry are investigated:

- the addition of a tangential velocity at the impact;
- the connection of a mass to more than two springs.

A tangential velocity is introduced in a spring-mass system. The goal is to show that the results of Section 1 still apply. The model to capture tangential velocity is as simple as possible, see Fig. 5. The impact law is such that the tangential

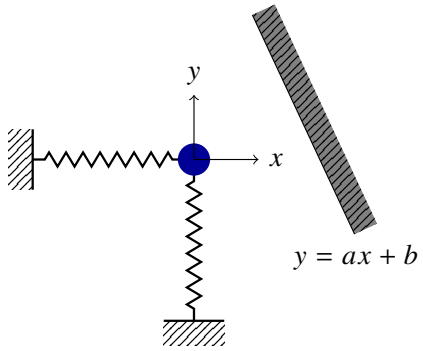

Figure 5. One mass with two degrees of freedom, subject to an elastic impact law.

component of the velocity is unchanged while the sign of its normal component is changed. This writes:

$$\vec{v}^+ = \vec{v}_\mathrm{t}^- - e\vec{v}_\mathrm{n}^- \tag{16}$$

where $^+$ ($^-$) denotes the post-impact (pre-impact) velocity. Eq. (16) can be expanded as

$$\begin{bmatrix}\dot{x}^+\\ \dot{y}^+\end{bmatrix} = \frac{1}{||\vec{t}||^2}([\dot{x}\ \dot{y}]\cdot\vec{t})\vec{t} - \frac{e}{||\vec{n}||^2}([\dot{x}\ \dot{y}]\cdot\vec{n})\vec{n} \tag{17}$$

$$= \underbrace{\frac{1}{1+a^2}\begin{bmatrix}1-ea^2 & a(1+e)\\ a(1+e) & a^2-e\end{bmatrix}}_{\mathbf{N}}\begin{bmatrix}\dot{x}^-\\ \dot{y}^-\end{bmatrix} \tag{18}$$

Note that the normal component of the velocity can be expressed in terms of the gap function $g(x, y)$ between the mass and the obstacle, equal to

$$g(x, y) = \frac{ax + b - y}{\sqrt{1 + a^2}} \tag{19}$$

This relation is $\vec{v}_\mathrm{n} = (\vec{\mathrm{grad}}\, g\cdot\vec{v})\vec{n}/||\vec{n}||$. With $e = 1$, $\mathbf{N}$ becomes

$$\mathbf{N} = \frac{1}{1+a^2}\begin{bmatrix}1-a^2 & 2a\\ 2a & a^2-1\end{bmatrix} \tag{20}$$

The eigenvalues of $\mathbf{N}$ are $+1$ and -1 (with corresponding eigenvectors $[1/a, 1]$ and $[-a, 1]$). Additionally, $\mathbf{N}$ is symmetric and involutory ($\mathbf{N}^2 = I$) hence is an orthogonal symmetry.

The matrix of change of basis which diagonalises $\mathbf{N}$ does not affect the diagonal nature of the mass matrix, provided its diagonal elements are equal to each other—condition which is fulfilled here. It is therefore possible to write the initial dynamical problem as an equivalent problem corresponding to a 2-dof spring-mass system in chain (as in Fig. 1). More precisely, the equivalent system has the same mass matrix; its stiffness matrix is the conjugation of the initial stiffness matrix with

$$\mathbf{P} = \begin{bmatrix} -a & 1/a \\ 1 & 1 \end{bmatrix} \tag{21}$$

and the new coordinates are given by $\mathbf{P} \cdot [x, y]^\top$. The problem hence falls within the context of the mathematical assumptions and results given in Section 1.

Complex models of aircraft engines are not unidimensional; one node can be connected to multiple neighbouring nodes, breaking the tridiagonal structure of the stiffness matrix. An example is illustrated in Figure 6. The stiffness matrix $\mathbf{K}$ is

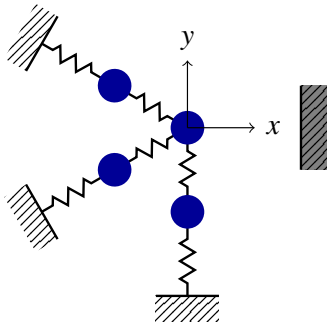

Figure 6. One mass connected to more than two other masses, breaking the tridiagonal structure of the stiffness matrix.

no longer tridiagonal but remains symmetric. Also, since $\mathbf{M}$ is diagonal, $\mathbf{M}^{-1}\mathbf{K}$ is also symmetric. It can therefore always be transformed in a tridiagonal matrix, leading to a spring-mass system in chain. The linear transformation affects the impact law but, from the previous result, the degrees-of-freedom of the contacting node can be rearranged to match with the generic system illustrated in Fig. 1.

The conclusion of this part is that the results extend to any spring-mass system—as long as its free flight exhibit linear dynamic behaviour. The key reason behind this is that any impact law written as an orthogonal symmetry with respect to a hyperplane can be diagonalised in an orthogonal basis where $\mathbf{M}^{-1}\mathbf{K}$ remains symmetric positive definite.

2.3 Scalability to large systems

Turbomachine models may include thousands degrees-of-freedom. It is natural to investigate how the results of Section 1 scale with the number of degrees of freedom. For motions with one impact per period, this is straightforward: for any T, expression (12) gives a potential solution which will be an actual solution if $x_n(t) \leq d$ for all t. For two impacts per period, solutions only exist for specific times of impact t_1, t_2 and an additional step is required to find such appropriate t_1, t_2. This consists in finding roots of the nonlinear equation (8) for $k = 2$. Computation times on a standard

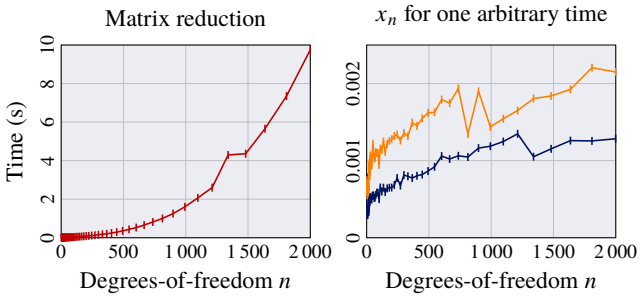

Figure 7. Computation time for construction of matrices of Section 1.2 and calculation of coordinates in phase space. [—] 1 ipp. [—] 2 ipp.

desktop PC are reported in Fig. 7 using the computer program Mathematica®. The left diagram shows the computation time for the matrix reduction, *i.e.* the calculation of the different matrices involved (namely: $\mathbf{M}$, $\mathbf{K}$, $\mathbf{B}$ and $\mathbf{Q}$). For a given number of degrees of freedom n, this is to be computed once. The right diagram shows the computation time of one coordinate in the state space, for a given time. Note that these timings would probably be reduced with a lower-level implementation and performance-tuning. Typical timing for 2000 dofs is 2 ms per coordinate. To approximate a nonlinear mode of a model with 2000 dofs with a few thousand states of the system would thus take a few seconds.

The conclusion of this subsection is that the number of degrees-of-freedom is not limiting for the computation of nonsmooth modes.

2.4 Sensitivity to number of dofs

It is natural to investigate the sensitivity of nonsmooth modes to the considered number of degrees-of-freedom. This is a challenging point: even for very large numbers of dofs, the existence of nonsmooth modes and their shape is extremely sensitive to n. An illustration is given in Fig. 8 where a mode exist in the neighbourhood of a period T when $n = 100$, while for the same T, the position calculated with formula (12) violates the constraint $x_n \leq d$ with $n = 101$, proving no mode locally exists around T. The reason for this is that existence of nonsmooth modes is largely determined by the harmonics (see denominators of Eqs. (3), (10), and (11). The set of the periods of all harmonics $\{2k\pi/\omega_i, k \in \mathbb{N}^*,\ i \in [\![1, n]\!]\}$ becomes so dense that the existence of nonsmooth modes is ensured only on very tiny domains in the impact times t_1, t_2. As opposed to linear modes, nonsmooth modes with an impact law do not converge with the number of degrees-of-freedom.

2.5 Behaviour of forced and damped system

Material fatigue can appear in turbomachines due to periodic forcing cycles. It can lead to failure and its prediction

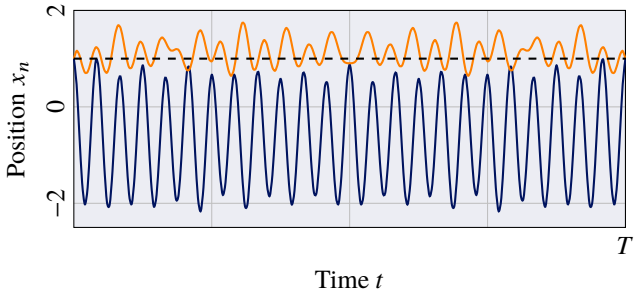

Figure 8. Non-convergence with respect to spatial discretization. Curves show the periodic motion of the n-th mass (1 ipp). For $n = 100$ [—], the position is an actual solution. For $n = 101$ [—], the position is completely different and is not even a solution: it violates the constraint $x_n \leq d$.

is therefore essential. In linear dynamics, the vibratory response to a periodic excitation is governed by the autonomous (*i.e.* unforced) response [8]. Vibratory resonance regimes are observed if the forcing frequency lies in the vicinity of the natural frequencies of the system. However, the superposition principle no longer applies when impacts are accounted for, making the response of nonsmooth systems under periodic forcing much more challenging to understand. Additionally, it is not known whether periodically-forced nonsmooth oscillators always exhibit a (periodic) steady-state regime. This subsection aims at comparing the energy of the nonsmooth modal responses to the periodically forced solutions of the same system under a purely sinusoidal force $F(t) = F_0 \cos(\Omega t)$ acting to every mass and a damping matrix simply chosen as $\mathbf{C} = \alpha \mathbf{K}$.

Using an event-driven algorithm [5], the time-evolution of the impact oscillator of Fig. 1 was calculated with $n = 5$ for several values of the excitation period $T = 2\pi/\Omega$. After 500 such periods, it was observed that the system usually had a periodic motion with 1 impact per period T, 2 impacts per period T or $2T$ or 3 impacts per period $2T$. For such periodic motions, the energy is plotted in Fig. 9. For the other ones, it is not known whether they could eventually reach the periodic regime.

It seems the peaks of energy for the forced systems (for $T \approx 2.4$) are almost aligned with the 1 ipp energy curve. Nevertheless, this observation cannot be generalised to all resonances of the nonsmooth modes. It is therefore not possible to conclude that resonance phenomena of forced systems always coincide with that of the nonsmooth modes. The response for two applied forces and two damping coefficients are shown in Fig. 10. Further investigations are required to capture the variety of the observed behaviours in motion and in energy.

2.6 Exploratory stability analysis

The question of stability is a common question in the analysis of dynamical systems. Indeed, it characterises the dynamics of a system in the vicinity of its fixed points or periodic orbits. For periodic orbits, Lyapunov stability is by the fact

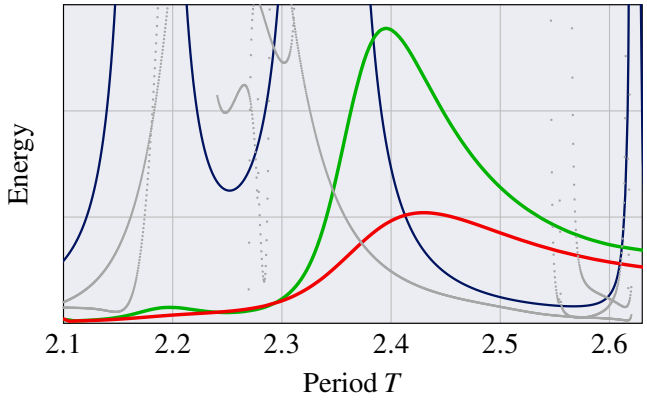

Figure 9. Energies of nonsmooth modes for 1 ipp [—] and 2 ipp [·····]. Energy of periodic solutions for the forced system with $F_0 = 1$, $\alpha = 0.005$ [—] and $\alpha = 0.01$ [—].

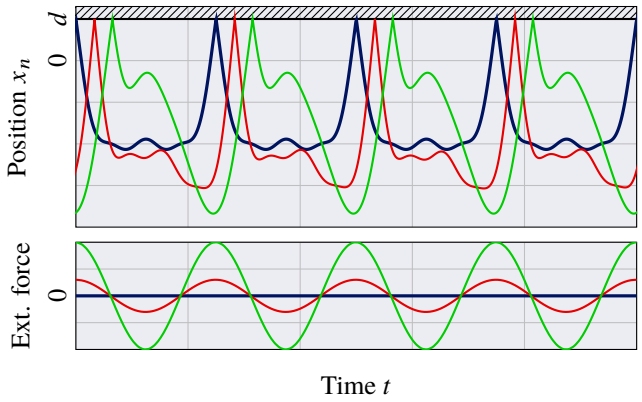

Figure 10. Two forced damped responses and the corresponding nonsmooth mode. [—] Nonsmooth mode. [—] $F_0 = 0.3$, $\alpha = 0.003$. [—] $F_0 = 1$, $\alpha = 0.03$.

that the response to any perturbation from a given periodic orbit remains in a neighbourhood or the periodic orbit [9]. Asymptotic stability is stronger and adds the condition that the system converges towards the orbit.

For smooth nonlinear systems, Lyapunov stability can be proven by linearising the dynamics in the neighbourhood of a known periodic solution. Similarly, here, the first points of the Poincaré section $x_n = d$ are plotted for a perturbed initial condition on the section. In other words, a point on the section corresponding to a nonsmooth mode (or more exactly, one periodic orbit on the manifold defining the mode) is selected. It is slightly perturbed (except the n-th position which is maintained equal to d) to provide an initial condition inserted in an event-driven algorithm to solve the dynamic equations: the dynamics is time-integrated and when $x_n = d$, the sign of the velocity $\dot{x}_n$ is inverted (Newton impact law). The time-integration then leads to a non-periodic trajectory. Every time the system hits the hyperplane $x_n = d$ in the state space, the pre-impact velocity $\dot{x}_n$ and the position x_{n-1} are collected. The obtained results are illustrated in Fig. 11 for $n = 5$.

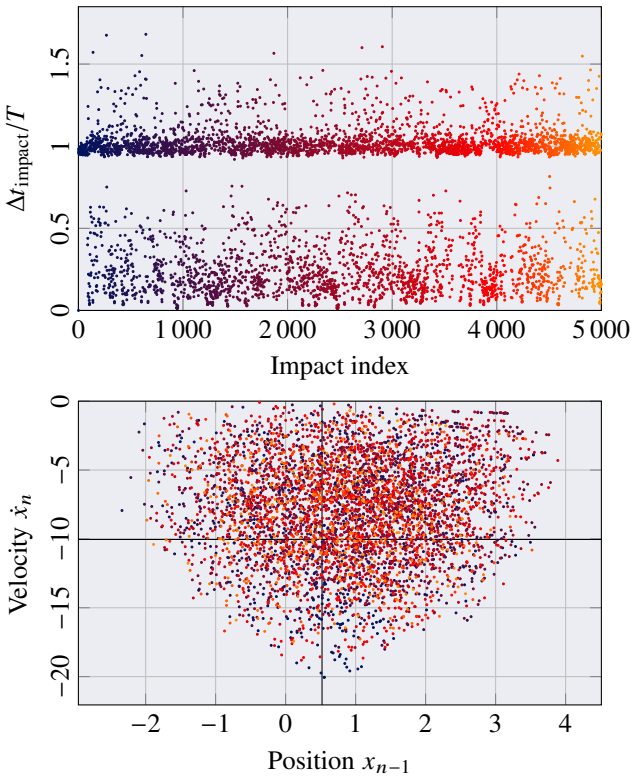

Figure 11. Motions with perturbated initial conditions. Top: Duration of the 5000 first free flights, normalised. Bottom: Poincaré section $x_n = d$.

First, it appears that the period T of the nonlinear mode plays an important role in the non-periodic motion with perturbed trajectories as depicted in Fig. 11, top. More than half of the 5000 free flights have a duration in $[0.9T, 1.1T]$. Second, the 5000 points of the Poincaré map appear to evolve in a fixed neighbourhood of the initial conditions. There is no tendency to move away from the neighbourhood with time: red and orange points are not particularly further from the center of Fig. 11 (bottom) than blue points. This behaviour has been observed for several numerical experiments, with various perturbations and n.

Although not a proof, these observations tend to indicate that orbits of nonsmooth modes are Lyapunov-stable, and not asymptotically stable.

CONCLUSION

The main mathematical results regarding nonsmooth modes, proven in a publication to come, are summarized. They prove existence and uniqueness, under some conditions, of periodic motions of an autonomous spring-mass chain, the last mass of which is subject to a Newton impact law. They also give the analytical expression of the solutions, when they exist and allow for an analytical calculation of nonsmooth modes with 1 impact per period, and approximation of nonsmooth modes for multiple impacts per period.

The goal of the present work is to identify possibilities and limitations to apply these results to the common blade–casing contact problem within turbomachines.

The existence of the fundamental skew-symmetric matrix Π, governing nonsmooth modes, was shown to be still ensured for non-diagonal mass matrices, opening doors to FEM applications. Also, the unidimensional geometry of the spring-mass chain proved not to be required for the results to hold, making the study of complex geometries possible, the limitation being that the impact law must have the form of a orthogonal symmetry with respect to a hyperplane. The computation time of a coordinate is about 2 ms for 2000 dofs without performance-tuning and on a standard PC, which is very reasonable and makes the study of complex turbomachines models conceivable. First numerical experiments tend to show that nonsmooth orbits are Lyapunov stable and not asymptotically stable.

Altogether, this investigation shows that the gap between the theoretical results for the specific spring-mass chain and real applications to turbomachines is not as wide as initially expected. However, some limitations remain. The first one is the possibly tremendous difference in shape between nonsmooth modes of two similar systems differing by a few degrees-of-freedom. This is explained by the extremely rich frequency range excited by impact events, and the underlying lack of convergence in space discretization. This is not an issue when the number of dof is fixed, as for example in a reduced-order model of a turbomachine where only specific modes of the complex structure are considered. The second current limitation is that the relationship between the energy-frequency graph of the forced system and its nonsmooth modes are not fully understood yet. Nonsmooth modal analysis can therefore not yet be used to predict the forced response of turbomachines and the forcing frequencies leading to high energy motions, when the forcing amplitude is too large.

REFERENCES

[1] R.M. Rosenberg. On nonlinear vibrations of systems with many degrees of freedom. *Advances in applied mechanics*, 9:155, 1966.

[2] S.W. Shaw and C. Pierre. Non-linear normal modes and invariant manifolds. *Journal of Sound and Vibration*, 150(1):170–173, 1991.

[3] G. Kerschen, M. Peeters, J.C. Golinval, and A.F. Vakakis. Nonlinear normal modes, part I: A useful framework for the structural dynamicist. *Mechanical Systems and Signal Processing*, 23(1):170–194, 2009.

[4] P. Almeida, C. Gibert, F. Thouverez, X. Leblanc, and J.-P. Ousty. Experimental analysis of dynamic interaction between a centrifugal compressor and its casing. *Journal of Turbomachinery*, 137(3):031008, 2015.

[5] V. Acary and B. Brogliato. *Numerical methods for nonsmooth dynamical systems: applications in mechanics and electronics*, volume 35. Springer, 2008.

[6] M. Legrand, S. Junca, and S. Heng. Nonsmooth modal analysis of a N degree-of-freedom system undergoing a purely elastic impact law. August 2015.

[7] A. Thorin, M. Legrand, and S. Junca. Nonsmooth modal analysis: Investigation of a 2-dof spring-mass system subject to an elastic impact law. In *International Design Engineering Technical Conferences & Computers and Information in Engineering Conference*, page 9, Boston, United States, August 2015. ASME.

[8] L. Meirovitch. *Methods of analytical dynamics*. Advanced engineering series. McGraw-Hill, 1970.

[9] J. Guckenheimer and P. Holmes. *Nonlinear oscillations, dynamical systems, and bifurcations of vector fields*, volume 42. Springer Science & Business Media, 1983.